

# Effect of Deformation on Surface Characteristics of Finite Metallic Crystals\*

V. V. Pogosov<sup>†</sup> and O. M. Shtepa

Department of Microelectronics, Zaporozhye National Technical University, Zaporozhye 69064, Ukraine

(Dated: March 22, 2022)

The surface stress and the contact potential differences of elastically deformed faces of Al, Cu, Au, Ni, and Ti crystals are calculated within the modified stabilized jellium model using the self – consistent Kohn–Sham method. The obtained values of the surface stress are in agreement with the results of the available first-principal calculations. We find that the work function decreases/increases linearly with elongation/compression of crystals. Our results confirm that the available experimental data for the contact potential difference obtained for the deformed surface by the Kelvin method do not correspond to the change of the work function but to the change of the surface potential. The problem of anisotropy of the work function and ionization potential of finite sample is discussed.

PACS numbers:

## I. INTRODUCTION

The preparation and study of nanometer scale structures attracts a considerable current interest for both technological and scientific reasons. The free-electron gas models are invariably popular tools in the physics of metals [1, 2] and low-dimensional structures [3].

Recently, several authors discussed the definition of the surface stress and the chemical potential for the case of finite samples [4, 5, 6, 7, 8].

In our previous papers [6, 8] we proposed a successful method to calculate the surface stress and the work function of a single elastically deformed finite metal crystal. It was applied for simple metal. A fairly tightly bound d band that overlaps and hybridizes with a broader nearly free – electron sp band characterizes transition metals. The cohesive properties of simple, noble and transition metals can be calculated from the first principles in the context of one-electron picture provided by the density-functional theory [9, 10].

The direct measurements, using the Kelvin method showed a decreasing/increasing of the contact potential difference (CPD) of the elastically tensed/compressed metal samples [11, 12, 13, 14]. A similar effect on CPD was observed at the surface of sample with a nonuniform distribution of residual mechanical stress [15]. The conventional method of measurement of the work function changes versus x-axes strain [11, 12, 13, 14] is based on the expression:

$$\Delta W_{Kel} \equiv W(u_{xx}) - W(0) = -CPD, \quad (1)$$

i.e., the work function as if increases for a tensed sample. The change  $\Delta W_{Kel}(u_{xx})$  was measured (see Fig.1) at the side perpendicular y- and z-directions,  $u_{xx}$  is the relative deformation along x-axes (see Fig.2). These, at first

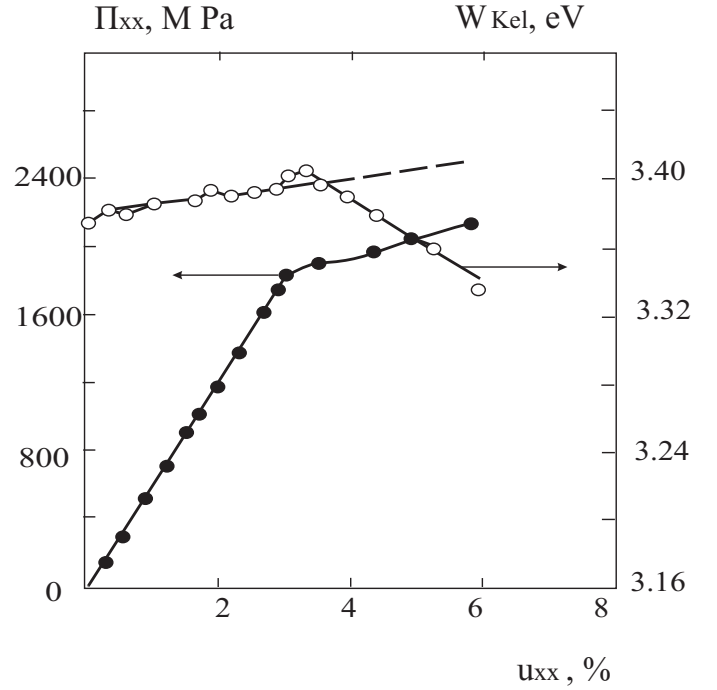


FIG. 1: The strain dependence of external mechanical stress  $\Pi_{xx}(u_{xx})$  and work function  $W_{Kel}(u_{xx})$ , defined by Eq.(1) for Al [13].

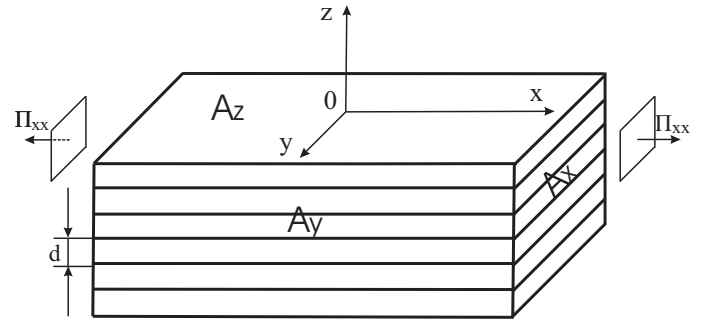


FIG. 2: Sketch of deformation.

\*Published in: Metallofiz. Noveishie Tekhnol. 2002 – **24** – P.1651-1656 (in parially); Ukr. Fiz. J. 2002 – **47** – P.1065-1071 (fully)

<sup>†</sup>Corresponding author: E-mail: vpogosov@zstu.edu.ua (V.V. Pogosov)

sight, surprising results mean that the work function in-

creases/decreases with uniaxial tension/compression of metallic sample. This fact contradicts to another well-known observation: the work function of simple metals decreases for the transition  $\text{Al} \Rightarrow \text{Na} \Rightarrow \text{Cs}$ , i.e. with decreasing of the electron concentration.

In the present paper, we report the results of calculations of the effect of deformation on the surface energy, the work function, and the contact potential difference of faces of technologically important metals such as Al, Ti, Ni, Cu, and Au using their nominal valence. The problem of an accurate definition of the work function is discussed. We checked the accuracy of Eq.(1) by fully self-consistent calculations and showed that it is wrong. Eq.(1) is incorrect in the diagnostic of strained surface.

## II. NONSTRAINED SURFACE

Surface energy per unit area and work function are the most important characteristics of a metal surface. In the framework of density-functional theory the total energy of metal is a functional of the nonhomogeneous electron concentration  $n(r)$ ,  $n(r) \Rightarrow \bar{n}$  in the bulk,  $\bar{n} = 3/4\pi r_{s0}^3$ ,  $r_{s0} = Z^{1/3}r_0$ ,  $r_{s0}$  and  $r_0$  are, respectively, the average between electron and between ion distances in the nonstrained metal bulk,  $Z$  is the metallic valence. Using a pseudopotential approach the total energy can be written as the sum

$$E[n(r)] = T_s + E_{ex} + E_{cor} + E_H + E_{ps} + E_M, \quad (2)$$

where  $T_s$  is the (non-interacting) electron kinetic energy,  $E_{ex}$  is the exchange energy,  $E_{cor}$  is the correlation energy,  $E_H$  is the Hartree (electrostatic) energy,  $E_{ps}$  is the pseudopotential correction, and  $E_M$  is the Madelung energy. The sum of first four terms in Eq.(2) corresponds to the energy of ordinary jellium,  $E_J$ . The ordinary jellium model provides a useful description for the bulk modulus and surface energy of the simple metals only for  $r_{s0} \approx 4$  bohr (Na), where bulk jellium is stable. The jellium surface energy for  $r_{s0} \leq 2$  and the bulk modulus for  $r_{s0} \geq 5$  bohr are negative. These deficiencies are removed in the stabilized jellium model [17]. The average energy per valence electron in the bulk of stabilized jellium is  $\bar{\varepsilon}_{SJ} = E[\bar{n}]/N$ , where  $N$  is a total number of free electrons, defined by valence and atomic density,

$$\bar{\varepsilon}_{SJ} = \bar{\varepsilon}_J + \bar{w}_R + \bar{\varepsilon}_M, \quad (3)$$

where the term ,

$$\bar{\varepsilon}_J = \bar{t}_s + \bar{\varepsilon}_{ex} + \bar{\varepsilon}_{cor} = \frac{3}{10}\bar{k}_F^2 + \frac{3}{4\pi}\bar{k}_F + \bar{\varepsilon}_{cor}, \quad (4)$$

consists of the average kinetic, exchange and correlation energy per electron,  $\bar{k}_F = (3\pi^2\bar{n}_0)^{1/3}$ ,  $r_0$  is the radius of the Wigner – Seitz cell, and  $w_R = 2\pi\bar{n}_0r_c^2$  represents the average of the repulsive part of the Ashcroft model potential,  $r_c$  is the radius of ionic core,  $\bar{\varepsilon}_M = -9Z/10r_0$ . We employ atomic units throughout ( $\hbar = m = e = 1$ )

and the popular expression for the correlation energy [18, 19]

$$\varepsilon_{cor}[n(r)] = \frac{0.1423}{1 + 0.8293n(r)^{-1/6} + 0.2068n(r)^{-1/3}}. \quad (5)$$

Applying the variation principle one can find the Euler – Lagrange equation for nonhomogeneous electron gas

$$\mu = V_{eff}(r) + \frac{\delta T_s[n]}{\delta n(r)}, \quad (6)$$

where  $\mu$  is the chemical potential of the electrons, and effective one – electron potential is

$$V_{eff}(r) = \varphi(r) + \frac{\delta[E_{ex} + E_{cor}]}{\delta n(r)} + \langle \delta V \rangle_{face} \theta(r - r'), \quad (7)$$

where  $r'$  is the radius-vector of the surface,  $\theta(r - r')$  is the step function. The electrostatic potential  $\varphi(r)$  satisfies the Poisson equation.

$$\nabla^2 \varphi(r) = -4\pi[n(r) - \rho(r)]. \quad (8)$$

The ionic charge distribution can be modelled by the step function  $\rho(r) = \bar{\rho}\theta(r - r')$ , where  $\bar{\rho} = \bar{n}_0/Z$ .

The coordinate-independent term  $\langle \delta V \rangle_{face}$  in Eq.(7) represents the difference between the pseudopotential of the ion lattice and the electrostatic potential of positive background averaged over the Wigner–Seitz cell. This term allows one to distinguish different faces of semi-infinite samples. The face-dependence of the stabilization potential [16, 17] reads

$$\langle \delta V \rangle_{face} = \langle \delta V \rangle_{WS} - \left( \frac{\bar{\varepsilon}_M}{3} + \frac{\pi\bar{n}_0}{6}d_0^2 \right), \quad (9)$$

$$\langle \delta V \rangle_{WS} = \bar{n}_0 \frac{d}{d\bar{n}_0} (\bar{\varepsilon}_M + \bar{w}_R), \quad (10)$$

where  $d_0$  is the spacing between the lattice planes parallel to the surface. From the bulk stability condition  $d\bar{\varepsilon}_{SJ}/d\bar{n}_0 = 0$  one can obtain the relation

$$\langle \delta V \rangle_{WS} = -\bar{n}_0 \frac{d}{d\bar{n}_0} (\bar{t}_s + \bar{\varepsilon}_{ex} + \bar{\varepsilon}_{cor}), \quad (11)$$

The electronic profile  $n(r)$  can be expressed in the terms of one-electron wave functions  $\psi_i$ ,

$$n(r) = \sum_{i=1}^N |\psi_i(r)|^2, \quad (12)$$

where the functions  $\psi_i$  satisfy the one-electron wave equation

$$-\frac{1}{2}\nabla^2 \psi_i(r) + V_{eff(face)}(r)\psi_i(r) = \varepsilon_i \psi_i(r). \quad (13)$$

The set of the Kohn-Sham equations must be solved self-consistently. Then the total kinetic energy of electrons in Eq.2 is

$$T_s[n] = \sum_{i=1}^N \varepsilon_i - \int d^3r n(r) V_{eff}(r) \quad (14)$$

As a rule for semi-infinite metal it is supposed that the electronic profile  $n(r)$  and effective potential  $V_{eff}(r)$  vary only in the direction perpendicular to the surface. The conventional approach involves introducing periodic boundary conditions in the x- and y-directions. Thus, only crystal face is in z-direction. In this case the set of equations (8), (12) and (13) reduces to

$$\varphi(z) = \varphi(\infty) - 4\pi \int_z^\infty dz' \int_{z'}^\infty dz'' [n(z'') - \rho(z'')], \quad (15)$$

$$n(z) = \frac{1}{\pi^2} \int_0^{\bar{k}_F} dk (\bar{k}_F^2 - k^2) |\psi_k(z)|^2, \quad (16)$$

$$\left[ -\frac{1}{2} \frac{d^2}{dz^2} + V_{eff}[z, n] \right] \psi_k(z) = \frac{1}{2} k^2 \psi_k(z). \quad (17)$$

Here the effective potential is taken in a local-density-approximation

$$V_{eff}[z, n] = \phi(z) + V_{xc}(z) + \langle \delta V \rangle_{face} \theta(-z), \quad (18)$$

where  $n \equiv n(z)$ . The electrons wave number varies in the interval  $(0, \bar{k}_F)$ . The solution of the problem can be reduced to the iteration procedure by means of the follow relation [20]

$$\phi_{i+1}(z) = \int_{-\infty}^\infty dz' e^{-k_F|z-z'|} \frac{2\pi}{k_F} [n(z') - \rho(z')] + \frac{k_F}{2} \phi_i(z), \quad (19)$$

where  $i$  is the number of iteration.

The surface energy can be written as

$$\gamma_{SJ} = \gamma_J + \langle V_{WS} \rangle \int_{-\infty}^0 dz [n(z) - \bar{n}_0], \quad (20)$$

The ordinary jellium components are:

$$\gamma_s = \frac{1}{2\pi^2} \int_0^{\bar{k}_F} dk k \left[ \frac{\pi}{4} - \delta(k) \right] - \int_{-\infty}^\infty dz n(z) [V_{eff(face)}(z) - \bar{V}_{eff(face)} \theta(-z)], \quad (21)$$

where  $\delta$  is the phase shift of wave function,  $\psi_k(z) \rightarrow \sin[kz - \delta(k)]$  as  $z \rightarrow -\infty$ ,  $\bar{V}_{eff(face)}$  is the bulk magnitude of effective potential, and

$$\gamma_{xc} = \int_{-\infty}^\infty dz [n(z) \varepsilon_{xc}(n(z)) - \bar{n} \varepsilon_{xc}(\bar{n}) \theta(-z)], \quad (22)$$

$$\gamma_H = \frac{1}{2} \int_{-\infty}^\infty dz \varphi(z) [n(z) - \rho(n(z))]. \quad (23)$$

Putting the electrostatic potential in the vacuum equal zero,  $\varphi(+\infty) = 0$ , one can calculate the work function as ( $\bar{\varepsilon}_F = \bar{k}_F^2/2$ )

$$W_{z-face} \equiv -\mu = -\bar{V}_{eff} - \bar{\varepsilon}_F. \quad (24)$$

### III. DEFORMED SURFACE

The strain dependence of the CPD was measured for polycrystalline compressed [11] and tensed samples [13, 14]. One can assume that a polycrystal is assembled from a number of simple crystallites. Thus, qualitatively, the problem can be reduced to an analysis of tension or compression applied to a single crystal. We consider a single crystal in the shape of a parallelepiped with sides having equivalent Miller indices. For simplicity, the material of the sample is assumed to have the cubic crystallographic symmetry. We introduce the coordinate system with axes and perpendicular to the sample faces. Their areas are equal to and respectively (see Fig.2). We neglect temperature and dimensional effects that differ from the approach used in [3, 21].

Let us first express the average electron density in a metal as a function of deformation. For this purpose, consider an undeformed cubic cell of side length  $a_0$ ,  $a_0^3 = 4\pi r_0^3/3$ . In the modified stabilized jellium model [6, 8] the metal energy is a function of the electron density parameter  $r_{su} = Z^{1/3} r_{0u}$ , spacing  $d_u$  between the lattice planes perpendicular to z-direction, the Poisson coefficient for polycrystal  $\nu$ , the Young modulus  $Y$ , and deformation  $u_{xx}$ .

For uniaxially deformed cell elongated or compressed along the x-axis one can write [8]:

$$d_u = d_0 (1 - \nu u_{xx}), \quad (25)$$

where  $d_u$  is the spacing between the lattice planes perpendicular to the y- or z-directions,  $d_0$  is the interplanar spacing in undeformed crystal,

$$\bar{n} = \bar{n}_0 [1 - (1 - 2\nu) u_{xx}] + O(u_{xx}^2), \quad (26)$$

is the average electron density in deformed metal bulk,  $\nu$  is the Poisson coefficient for polycrystal and the corresponding density parameter is .

$$r_{su} = r_s [1 + (1 - 2\nu) u_{xx}]^{1/3}. \quad (27)$$

The stabilization potential (11) must be changed by

$$\langle \delta V \rangle_{WS} = -\bar{n}_0 \frac{d}{d\bar{n}_0} \left( \bar{t}_s + \bar{\varepsilon}_{ex} + \bar{\varepsilon}_{cor} + \frac{P}{\bar{n}_0} \right), \quad (28)$$

where

$$P = -(\Pi_{xx} + \Pi_{yy} + \Pi_{zz}) = -Y u_{xx} (1 - 2\nu)$$

is the external pressure.

An applied force stimulates the change of a volume and reticular electron density at particular faces of neutral metallic crystal and results in a difference between electrostatic potentials of these faces.

The corresponding anisotropic three-dimensional electric field arises due to a transfer of electrons between faces. Thus, finite sample sizes lead, in the first place, to the fact that the surface tends to equipotentiality. In general case, this transfer of electrons does not give any possibility to calculate the work function using conventional approach for semi-infinite sample. However, in the special case of the largest face of the metallic crystal,

$$A_z \gg A_x, A_y, \quad (29)$$

the use of the conventional approach (see Eq. (24)) in fact is adequate [8],  $A_z$  is the area of upper side at Fig. 2. As a result, the calculated work function exclusively for  $z$ -direction corresponds to that for the *whole* crystal. The face perpendicular to this direction is not appreciably perturbed by the transferred electronic charge independently from the crystallographic orientation [8]. The conventional method involves introducing periodic boundary conditions in the  $x$ - and  $y$ -directions. In this case the surface potential depends strongly from the atomic packing density. Thus, the only crystal face is in  $z$ -direction. Putting the three-dimensional electrostatic potential in the vacuum equal zero, under condition (29) one can use definition (24), where the effective potential in the bulk of semi-infinite metal yields the total sample-vacuum barrier. Solving the set of Eqs. (15) – (18) and using relations (25) – (28), one can calculate the strain dependencies of the surface energy and work function.

We calculate the diagonal component of surface stress for given largest face using the following expression [5, 6, 7, 8]:

$$\tau_{xx} = \gamma + \frac{d\gamma}{du_{xx}}, \quad (30)$$

where  $\gamma$  is the surface energy per unit area of the largest face of sample.

#### IV. RESULTS AND DISCUSSIONS

We performed our calculations for the work function and the surface energy for the case of absence of the strain state of metals and for the strain dependences

TABLE I: Calculated bulk modulus  $B$ , surface energy  $\gamma_{face}$ , and the work function  $W_{face}$ . For univalent Au ( $Z = 1$ ) the results are placed in brackets. The experimental values of  $B$  (are given),  $\sigma$ ,  $W_{face}$  for polycrystalline metal, and the Poisson ratio  $\nu$ , the Young modulus  $Y$  necessary for calculation the strain dependences are taken from books [23, 24, 25].

	$B$ [Mbar]	Face	$\sigma_{face}$ [erg/cm <sup>2</sup> ]	$W_{face}$ [eV]	$Y$ [GPa]	$\nu$
Al	1.565/0.722	(100)	1087	3.806	62.5	0.34
		(110)	1683	3.643	71.4	
		(111)	939	4.119	75.1	
Au	1.519(0.202)/0.722	(100)	1069(395)	3.792(3.318)	43.5	0.42
		(110)	1652(440)	3.630(3.148)	81.3	
		(111)	924(383)	4.105(3.478)	115.0	
Ni	2.567/1.860	(100)	1376	4.010	138.0	0.32
		(110)	2224	3.858	215.0	
		(111)	1162	4.325	262.0	
Cu	1.113/1.370	(100)	979	3.855	65.8	0.35
		(110)	1295	3.647	131.0	
		(111)	899	4.123	194.0	
Ti	1.565/0.722	(0001)	1081	4.205	145.0	0.30
		(100)	1355	3.865	96.1	
		(110)	2456	3.774	96.1	
		(111)	1081	4.205	27.8	

$W_{face}(u_{xx})$  and  $\gamma_{face}(u_{xx})$  within the range of deformation  $-0.01 \leq u_{xx} \leq +0.01$  for Ni and  $-0.03 \leq u_{xx} \leq +0.03$  for Al, Au, Cu, and Ti, respectively. The positive/negative deformation is equivalent to the tension/compression of the largest side of the sample, i.e., the decrease/increase of the atomic packing density at this side, and the decrease/increase of the mean electron concentration and the interplanar spacing in direction. Upper side of sample in Fig.2 is suggested as having indexes (100), (110), (111) or (0001).

The trends in bulk and surface characteristics of Al, Au, Cu, Ni, and Ti have been reproduced from the theory of uniform electron gas with the average electron density corresponding to the nominal valence by the volume per atom. The use of the integer and fractional magnitude of a valency leads to a successful calculation of bulk modulus  $B$  [22]. The concept of the metallic valency can be defined to treat simple and transition metals in terms of the uniform electron gas.

The results of our calculations for free and deformed faces are summarized in Table I and Figs.2 and 3, respectively. For comparison we perform calculations of bulk modulus  $B = \bar{n}_0^2 d^2(\bar{n}_0^2 \bar{\varepsilon}_{SJ}) / d\bar{n}_0^2$ ,  $\gamma$  and  $W$  for Au ( $Z = 1$ ). The data of Table I demonstrate intricate picture for common description of cohesive and surface metallic properties in the simple approach. In fact the use of nominal valence gives satisfactory results for the surface characteristics. We found that the deformation changes

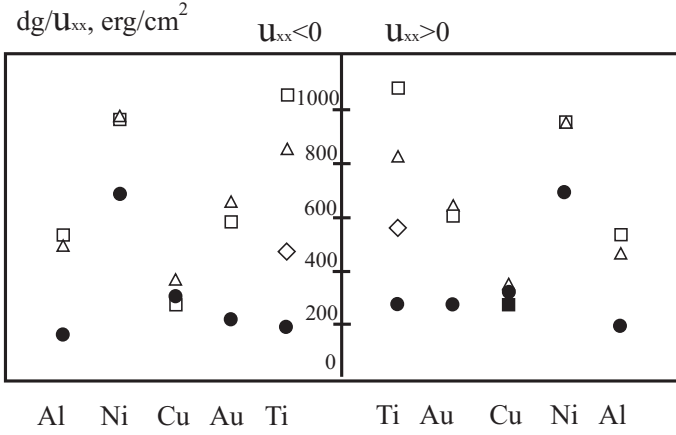


FIG. 3: Calculated derivative  $d\gamma/du_{xx}$  for estimation of the surface stress, Eq.(29). The left and right parts of the figure correspond to the compression ( $u_{xx} < 0$ ) and the tension ( $u_{xx} > 0$ ) of the sample, respectively:  $\square$  – fcc (100),  $\triangle$  – fcc (110),  $\bullet$  – fcc (111),  $\diamond$  – hcp (0001).

of the work function and the surface energy remain linear with respect to the deformation. The strain derivative of the work function and the surface energy is positive. The values of surface stress component vary appreciably within the interval  $(1.15, 1.75)\gamma_{face}$ . Similar results for the surface stress (1250 and 1440 erg/cm<sup>2</sup> for Al (111)) are yielded by the *ab initio* [26] and atomistic [27] calculations. In contrast to the present work (Fig.3), the strain derivative obtained for Au in [28] was larger than the surface energy.

The relative change of the work function equals approximately 1% for the maximal strains (compare Table I and Fig.4). For the case of the compression ( $u_{xx} < 0$ ), the tail of electron profile and, therefore, of the effective potential grows steeper in vacuum. For the case of the tensile strain ( $u_{xx} > 0$ ), these coordinate dependences have the opposite tendency. A total decrease/increase of the work function is determined by a positive/negative shift of the effective potential versus strain in the bulk of metal (neglecting the deformation dependence  $\varepsilon_F(u_{xx})$ , one can certainly put the shift  $\Delta W \simeq -\Delta\bar{V}_{eff}$ ). Our calculation mimics the usual work function dependence from electronic concentration (for transition  $\text{Al} \Rightarrow \text{Na} \Rightarrow \text{Cs}$ ).

However, relation (1) gives incorrect dependence  $W(u_{xx})$ . These results, at first sight, contradict to experiments [11, 12, 13, 14].

We suggest that, qualitatively, the problem is reduced to the effect of strain on a single crystal. The experimental observations can be explained based on the change of the effective potential at the position of the image plane  $z = z_0$  [8]. For simplicity we take  $z_0 = 1$  bohr for faces and use

$$CPD = \Delta V_{eff}(z_0, u_{xx}).$$

At present, we calculated  $\Delta W$  and  $CPD$  without use of Eq.(1). Our Fig.4 demonstrates, on the one hand, a good

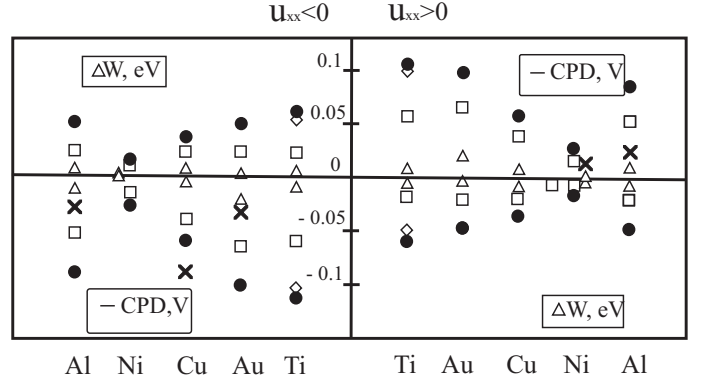


FIG. 4: Calculated change of the work function and the contact potential difference for maximal strain of elastically deformed largest faces (Fig.2). The experimental values of  $-CPD$  taken from [11] for compressed ( $u_{xx} = -0.03$ ) polycrystalline Al, Cu, and Au samples, and from [13, 14] for tensed Al ( $u_{xx} = +0.03$ ) and Ni ( $u_{xx} = +0.01$ ) samples (see also Table 1 in [29]). The values of for negative deformation are extracted from the lowest experimental shifts in contact potential  $-CPD$  (measured in units of  $\mu\text{V} \times \text{cm}^2/\text{kg}$ ) of [11] multiplied by  $\bar{Y}|u_{xx}|$ , where  $\bar{Y} = \frac{1}{3}(Y_{001} + Y_{110} + Y_{111})$ . Note that the values of and were erroneously equated in [11, 12, 13, 14, 15].

qualitative agreement of the calculated values of with the experimental data, on the other hand, the inverse dependence than it follows from Eq. (1).

Let us introduce  $\xi$  the ratio of the effective potential differences between strained and strain-free samples at the surface and in the bulk,

$$\xi = \frac{\Delta V_{eff}(z_0, u_{xx})}{\Delta V_{eff}(u_{xx})} \simeq \frac{CPD}{-\Delta W},$$

where  $\bar{V}_{eff}(u_{xx}) \equiv V_{eff}(z = -\infty, u_{xx})$ . The calculations show that the value  $\xi$  varies within the interval  $(-3, -1)$  for the metal faces under study. For Al  $\xi \simeq -2.8!!!$

The analysis of experimental data provided the evidence that it is not adequate to use the Kelvin method for the measurement, e.g., of temperature dependence of the work function (see Fig. 6 of [30]).

Our results show:

- (i) the strain changes of the effective potential in the bulk and at the surface have the *opposite signs*,
- (ii) the sign of the deformation effect is *independent* on the material and of the crystallographic orientation.

In the conclusion let us remember that the density-functional calculations of this quantity deal with the nonrealistic semi-infinite systems. However, in all experiments *finite* samples are used, in general, of arbitrary sizes and shapes. In this context, an important remark appears about the conventional definition of face-dependent work function. The ionization potential (*IP*) of a finite sample (as a giant molecule) is given by

$$IP = E_{N-1} - E_N \simeq W + \frac{e^2}{2C}, \quad (31)$$

where  $E_N$  is the total energy of neutral metallic sample containing  $N$  electrons. Here  $W$  is introduced as a work function of the *whole* sample and  $C$  is a capacitance of the sample, which is a scalar quantity. It is clearly seen from Eq.(31) that the work function is not an anisotropic characteristic but a scalar quantity, and  $IP \rightarrow W$  at  $C \rightarrow \infty$ . It may be demonstrated by formation of finite sample adding consistently atoms each to other. The ionization potential of single atom, dimer, etc. (up to work function) corresponds to the ionization process of each stage of nucleation (up to the solid) [31]. Thus, the conventional definition (31) leads to the conclusion that the concept of an anisotropy of the work function of metal is spurious in principle. Hence, the realistic geometry considerations presented in the [16, 32] are adequate in

the case when all sample faces possess the same atomic packing density.

Our theory can be applied for the explanation of new pressure effects in a single-electron transistor [33].

### Acknowledgments

This work was supported by the Ministry of Education and Science of Ukraine and the NATO Science for Peace Programme. We thank Prof. V. U. Nazarov for giving us an access to his computer code for testing purposes and Dr. W. V. Pogosov for reading the manuscript.

- 
- [1] Sahni V., Solomatin A. // Adv. Quant. Chem.- 1999.- **33**.- P.241 - 271.
  - [2] Shore H.B., Rose J.H. // Phys. Rev.- 1999.- **B59**.- 16.- P.10458 - 10492.
  - [3] Pogosov V.V., Kotlyarov D.P., Kiejna A., Wojciechowski K.F. // Surf. Sci.- 2001.- **472**.- P.172 - 176.
  - [4] Pogosov V.V., Pogosov W.V., Kotlyarov D.P. // Zh. Eksp. Teor. Fiz.- 2000.- **117**.- 5.- P.1043 -1053.
  - [5] Sanfeld A., Steinchen A. // Surf. Sci.- 2000.- **463**.- P.157 - 173.
  - [6] Kiejna A., Pogosov V.V. // Phys. Rev.- 2000.- **B62**.- 15.- P.10445 - 10450.
  - [7] Bottlomey D.J., Ogino T. // Phys. Rev.- 2001.- **B63**.- P.165412.
  - [8] Pogosov V.V., Kurbatsky V.P. // Zh. Eksp. Teor. Fiz.- 2001.- **119**.- P.350-358.
  - [9] Moruzzi V.L., Jenak J.F., Williams A.R. *Calculated Electronic Properties of Metals*.- New York: Pergamon, 1978.
  - [10] Wills J.M., Harrison W.A. // Phys. Rev.- 1983.- **B28**.- P.4363 - 4368.
  - [11] Craig P.P. // Phys. Rev. Lett.- 1969.- **22**.- P.700 - 703.
  - [12] Mints P.I., Melekhin V.P., Partensky M.B. // Fizika Tverd. Tela.- 1974.- **16**.- P.3584 - 3586.
  - [13] Pogosov V.V., Levitin V.V., Loskutov S.V. // JTP Lett.- 1990.- **16**.- P.14 - 17.
  - [14] Loskutov S.V. // Fiz. Met. i Metalloved.- 1998.- **86**.- 2.- P.149 - 152.
  - [15] Levitin V.V., Loskutov S.V., Pravda M.I., Serpetsky B.A. // Nondestr. Test. Eval.- 2001.- **17**.- P.79 - 89.
  - [16] Lang N.D., Kohn W. // Phys. Rev.- 1971.- **B3**.- P.1215 - 1223.
  - [17] Perdew J.P. // Prog. Surf. Sci.- 1995.- **48**.- P.245 - 259.
  - [18] Ceperley D.M., Alder B.J. // Phys. Rev. Lett.- 1980.- **45**.- P.510 - 515.
  - [19] Perdew J.P., Zunger A. // Phys. Rev.- 1981.- **B23**.- P.5048 - 5055.
  - [20] Manninen M., Nieminen R., Hautajarvi P., Arponen J. // Phys. Rev.- 1975.- **B12**.- 10.- P.4012 - 4022.
  - [21] Pogosov V.V., Kotlyarov D.P., Mileschkina N.V., Kalganov V.D., Deck T., Moscardini A. // Phys.Low-Dimen. Struc.- 2000.- **7/8**.- P.91 - 104.
  - [22] Wojciechowski K. // Physica.- 1996.- **B229**.- P.55 - 62.
  - [23] Fomenko V.S. *Emission Properties of Metals*.- Kiev: Naukova Dumka, 1980.
  - [24] *Tables of Physical Values*. edited by I.K. Kikoin.- Moscow: Atomizdat, 1976.
  - [25] de Boer F.R., Boom R., Mattens W.C.M., Miedema A.R., Niessen A.K. *Cohesion in Metals*.- Amsterdam: North-Holland, 1988.
  - [26] Needs R.J., Godfrey M.J. // Phys. Rev.- 1990.- **B42**.- P.10933 - 10940.
  - [27] Feibelman P.J. // Phys. Rev.- 1994.- **B50**.- P.1908 - 1913.
  - [28] Needs R.J., Mansfield M. // J. Phys.: Condens. Matter.- 1989.- **1**.- P.7555 - 7566.
  - [29] Pogosov V.V. // Sol. St. Commun.- 1992.- **81**.- P.129 - 133.
  - [30] Durakiewicz T., Arko A.J., Joyce J.J., Moore D.P., Halas S. // Surf. Sci.- 2001.- **478**.- P.72 - 82.
  - [31] Frenkel Ya.I. *Introduction in the theory of metals*. Chapter 2.- Moscow: GIFML, 1958.
  - [32] Smoluchowski R. // Phys. Rev.- 1941.- **60**.- P.661 - 674.
  - [33] Kitada M. <http://lt.px.tsukuba.ac.jp/users/kitada/masterthesis.pdf>